AIP | The Journal of Chemical Physics

Change of translational-rotational coupling in liquids revealed by field-cycling 1H NMR

R. Meier, E. Schneider, and E. A. Rössler

Citation: The Journal of Chemical Physics **142**, 034503 (2015); doi: 10.1063/1.4904719
View online: http://dx.doi.org/10.1063/1.4904719
View Table of Contents: http://scitation.aip.org/content/aip/journal/jcp/142/3?ver=pdfcov
Published by the AIP Publishing

Change of translational-rotational coupling in liquids revealed by field-cycling ^{1}H NMR

R. Meier, E. Schneider, and E. A. Rössler
Experimentalphysik II, Universität Bayreuth, D-95440 Bayreuth, Germany

(Received 10 October 2014; accepted 8 December 2014; published online 20 January 2015)

Applying the field-cycling nuclear magnetic resonance technique, the frequency dependence of the ^{1}H spin-lattice relaxation rate, $R_1(\omega) = T_1^{-1}(\omega)$, is measured for propylene glycol (PG) which is increasingly diluted with deuterated chloroform. A frequency range of 10 kHz–20 MHz and a broad temperature interval from 220 to about 100 K are covered. The results are compared to those of experiments, where glycerol and *o*-terphenyl are diluted with their deuterated counter-part. Reflecting intra- as well as intermolecular relaxation, the dispersion curves $R_1(\omega, x)$ (x denotes mole fraction PG) allow to extract the rotational time constant $\tau_{rot}(T, x)$ and the self-diffusion coefficient $D(T, x)$ in a single experiment. The Stokes-Einstein-Debye (SED) relation is tested in terms of the quantity $D(\mathrm{T}, x)\tau_{rot}(\mathrm{T}, x)$ which provides a measure of an effective hydrodynamic radius or equivalently of the spectral separation of the translational and the rotational relaxation contribution. In contrast to *o*-terphenyl, glycerol and PG show a spectral separation much larger than suggested by the SED relation. In the case of PG/chloroform mixtures, not only an acceleration of the PG dynamics is observed with increasing dilution but also the spectral separation of rotational and translational relaxation contributions continuously decreases. Finally, following a behavior similar to that of *o*-terphenyl already at about x = 0.6; i.e., while $D(T, x)\tau_{rot}(T, x)$ in the mixture is essentially temperature independent, it strongly increases with x signaling thus a change of translational-rotational coupling. This directly reflects the dissolution of the hydrogen-bond network and thus a change of solution structure. © *2015 AIP Publishing LLC.* [http://dx.doi.org/10.1063/1.4904719]

INTRODUCTION

Nuclear magnetic resonance (NMR) relaxometry is a well established method accessing important information on molecular dynamics in condensed matter, especially in liquids and polymer melts. In particular, the field-cycling (FC) technique allows to measure the frequency dependency (dispersion) of the spin-lattice relaxation rate $R_1(\omega) = T_1^{-1}(\omega)$ by systematically varying the relaxation field.[1–3] The method has gained new momentum with the availability of a commercial FC relaxometer typically operated in the frequency range of 10 kHz–20 MHz (for ^{1}H).[1] Employing earth field compensation, even frequencies down to 100 Hz can be reached.[4–7] In most cases, the FC method is applied to protons and the relaxation is induced by fluctuations of the magnetic dipole-dipole interaction, and one has to distinguish intra- and intermolecular relaxation contributions.[1,3,7,8] While the first reflect reorientational dynamics the latter are mediated also by translational dynamics. In a series of papers, we have shown that the translational dynamics dominates the dispersion at low-frequencies.[3,9–13] In other words, rotational and translational relaxation contributions are spectrally separated. Due to the fact that at long times diffusion in liquids is of Fickian character a universal low-frequency dispersion law holds enabling the determination of the diffusion coefficient $D(T)$ as an alternative method to field gradient (FG) NMR. Although the ideas have been around in the literature since long,[14–17] their application has become easily possible with the recent relaxometers. The approach can be applied to the total ^{1}H relaxation without explicit separation of intra- and intermolecular relaxation, for example, via an isotope dilution experiment.[10,12,18–20] Thus, a full relaxation analysis yields both the rotational time constant τ_{rot} as well as D with a single FC ^{1}H NMR experiment. The product $D\tau_{\mathrm{rot}}$ is a measure of the extent of the spectral separation of rotational and translational relaxation contributions, i.e., a measure of the ratio $\tau_{\mathrm{trans}}/\tau_{\mathrm{rot}}$. In the frame of a hydrodynamic description, the quantity $D\tau_{\mathrm{rot}}$ provides the square of an effective hydrodynamic radius.

At high frequencies beyond the limit of the universal dispersion law, the particular frequency dependence of the rate $R_1(\omega)$ depends on the extent of spectral separation of the translational and rotational relaxation contribution as well as on the strengths of the intra- and intermolecular dipole-dipole couplings. As said, the intra- and intermolecular relaxations can be explicitly separated by applying the isotope dilution technique. Here, one dilutes protonated molecules in their deuterated counterpart, and as the ^{1}H-^{2}H dipole–dipole coupling is much weaker than the ^{1}H-^{1}H coupling,[8,20] the intermolecular contribution to the total relaxation decreases with decreasing the mole fraction x of the protonated molecules. Here, it is assumed that the dynamics in the mixture is not altered; only the intermolecular dipole-dipole coupling is reduced. Yet, one can also dilute a protonated liquid with a chemically different deuterated liquid. Consider the hydrogen-

bonded liquids glycerol or propylene glycol (PG). Diluting these liquids with some non-associating deuterated liquid like chloroform, for example, the dynamics will not only be changed in terms of the time constants $\tau_{rot}(x)$ and $D(x)$ but also the product $D\tau_{rot}$, i.e., the extent of spectral separation of reorientational and translational relaxation contribution will change, since, as will be demonstrated, in the present example the hydrogen-bond network of PG is successively destroyed by adding chloroform. There are innumerable studies testing the behavior of the quantity $D\tau_{rot}$, for instance, in terms of the Stokes-Einstein-Debye (SED) relation; however, usually different experimental techniques have to be combined. In particular, the temperature dependence of $D\tau_{rot}$ in super-cooled liquids gained attention in terms of enhanced translational diffusion occurring close to the glass transition temperature T_g.[21,22] In the present contribution, we do not reach such low temperatures and stick to the fluid-to-moderately viscous liquid state, i.e., to temperatures well above T_g.

Analyzing the relaxation dispersion of mixtures PG/chloroform-d_1 over a large concentration and temperature range we will first demonstrate how $\tau_{rot}(x,T)$ and $D(x,T)$ change upon dilution and cooling. Second, the evolution of $D\tau_{rot}$ with mole fraction, x, will provide insight into the changing association of the PG molecules (forming a hydrogen bond network in neat PG) in the mixture with chloroform. Thus, in terms of the SED relation, the hydrodynamic radius changes as a function of x directly reflecting the changing solution structure. The data will be compared with previous FC ^{1}H NMR results for the mixtures glycerol-h_5/glycerol-d_8[10] and *o*-terphenyl/*o*-terphenyl-d_{14} (OTP)[12] for which a change of $D\tau_{rot}$ is not expected.

THEORETICAL BACKGROUND

The total spin-lattice relaxation rate, $R_1(\omega)$, consists of an intramolecular part, $R^{rot}_{1,intra}(\omega)$, which is determined by rotational dynamics and an intermolecular part mediated by both rotational and translational motion.[10,12,23,24] Thus, one has to distinguish between intermolecular relaxation due to pure translation, $R^{trans}_{1,inter}(\omega)$, and due to rotation, $R^{rot}_{1,inter}(\omega)$, the latter is caused by the so-called eccentricity effect, i.e., when the spins are not placed in the molecules' center.[23,24] It has been shown that the three relaxation paths contribute additively to the total rate $R_1(\omega)$[10,12]

$$R_1(\omega) = R^{rot}_{1,intra}(\omega) + R^{rot}_{1,inter}(\omega) + R^{trans}_{1,inter}(\omega). \quad (1)$$

The intermolecularly mediated translational contribution is given by

$$R^{trans}_{1,inter}(\omega) = \frac{K_{inter}}{5}[J_{trans}(\omega) + 4J_{trans}(2\omega)], \quad (2)$$

and the normalized spectral density $J_{trans}(\omega)$ is described in reasonable approximation by the force-free-hard-sphere (FFHS) model[15,16]

$$J_{trans}(\omega) = \frac{54}{\pi}\int_0^\infty \frac{u^2}{81+9u^2-2u^2+u^6}\frac{u^2\tau_{trans}}{u^4+(\omega\tau_{trans})^2}du, \quad (3)$$

and with K_{inter} given by

$$K_{inter} = \frac{8\pi}{3} I_H(I_H+1)\frac{N_H}{d^3}\left(\frac{\mu_0}{4\pi}\hbar\gamma_H^2\right)^2, \quad (4)$$

in which γ_H is the ^{1}H gyro-magnetic ratio, I_H the spin quantum number, and N_H the ^{1}H spin density. Within the FFHS model, the quantity d describes the distance of closest approach of two spins and can be interpreted as a measure of the molecule's diameter. The translational time constant is defined as $\tau_{trans} = d^2/2D$ with D being the self-diffusion coefficient.[8,15,16]

Again, following our previously introduced phenomenological analysis, the total rotational contribution reads[10,12]

$$R^{rot}_1(\omega) = R^{rot}_{1,intra}(\omega) + R^{rot}_{1,inter}(\omega) = \frac{(K_{intra} + f\cdot K_{inter})}{5}\cdot[J_{rot}(\omega) + 4J_{rot}(2\omega)]. \quad (5)$$

The impact of the eccentricity effect is accounted for by the parameter f. The rotational dynamics in dense liquids is described by a Cole-Davidson (CD) spectral density as is well confirmed by dielectric spectroscopy and dynamic light scattering[25,26]

$$J_{rot}(\omega) \equiv \frac{\sin[\beta\cdot\arctan(\omega\tau_{CD})]}{\omega\cdot\left[1+(\omega\tau_{CD})^2\right]^{\frac{\beta}{2}}}. \quad (6)$$

The corresponding rotational time constant is given by $\tau_{rot} = \beta\tau_{CD}$, and for the intramolecular coupling constant K_{intra} holds $R^{rot}_{1,intra}(0) = K_{intra}\cdot\tau_{rot}$.

Here, a note is worthwhile. We are well aware that assuming rotational and translational (small-step) diffusion as done in the work of Ayant *et al.*,[23] the intermolecular rate involves an infinite sum of products of rotational and translational correlation functions of increasing rank. Yet, in a recent analysis,[12] we have shown that phenomenologically the dispersion spectra of the eccentricity model of Ayant *et al.* can be approximately separated into two terms, namely a translational part given by Eq. (3) and a rotational part given by a CD function and weighted by a factor f (cf. Eq. (5)). Thus, as was also tested experimentally,[10,12] the total relaxation is well approximated by Eq. (1), and we will demonstrate that the extracted quantities (e.g., the hydrodynamic radii) well agree with those from literature.

As has been demonstrated, the low-frequency dispersion of the total relaxation rate $R_1(\omega)$ is dominated by the translational motion which yields in leading order a universal dispersion[3,11,14–17]

$$R_1(\omega) = R_1(0) - \frac{B}{D^{3/2}}\cdot\sqrt{\omega}, \quad (7)$$

with

$$B = \frac{2\pi}{45}\left(1+4\sqrt{2}\right) I_A(I_A+1)N_H\left(\frac{\mu_0}{4\pi}\hbar\gamma_H^2\right)^2 \quad (8)$$

and

$$R_1(0) = (K_{intra} + f\cdot K_{inter})\cdot\tau_{rot} + \frac{4}{9}K_{inter}\tau_{trans}. \quad (9)$$

The $R_1(0)$ obtained by extrapolating $R_1(\omega)$ to zero frequency along Eq. (7) contains contributions from both rotationally as well as translationally mediated relaxations. In a mixture of protonated and deuterated liquids with a spin density,

$N_H = N_0 x$, where N_0 denotes the ^{1}H density of the pure protonated liquid and x refers to the mole fraction of the protonated liquid, one can extract the self-diffusion coefficient, $D(T)$, from the slope $m = dR_1/d\sqrt{\omega}$ of the rate dispersion at low frequencies. A comparison with FG NMR results demonstrated excellent agreement (cf. again Fig. 7).[11–13]

In previous works, we transformed the dispersion data measured at different temperatures into the susceptibility representation $\chi''(\omega) = \omega R_1(\omega)$. Starting from low temperatures for which rotational dynamics dominate the relaxation and applying frequency-temperature superposition (FTS), master curves $\chi''(\omega\tau_{rot})$ were obtained.[2,3,27,28] This procedure provides $\tau_{rot} = \tau_{rot}(T)$. In contrast, on the basis of the universal low-frequency dispersion law (Eq. (7)), it is possible to provide master curves directly for the relaxation rate; i.e., a spectral density is rescaled along the functional dependence[3,12,13]

$$R_1(\omega)/R_1(0) = 1 - \sqrt{\omega\tau_{res}}, \tag{10}$$

with a time constant τ_{res} connected to the diffusion coefficient D

$$\tau_{res} = \left(\frac{B}{D^{3/2} \cdot R_1(0)}\right)^2. \tag{11}$$

When translational-rotational coupling holds, i.e., the spectral separation of translational and rotational contributions in the dispersion data quantified by $r = \tau_{trans}/\tau_{rot}$ is independent of temperature, the such obtained master curve coincides also at higher frequencies, where the linearity in $\sqrt{\omega}$ ceases to hold. The shape of the master curves in terms of Eq. (10) gives information on the extent of the spectral separation r.[12] Explicitly, when the master curve leaves the linear regime in a downwards direction, r is most likely small and approximately fulfills the condition $r = 9$ following from the SED relation, i.e., assuming that a hydrodynamic sphere rotates and translates in a viscous medium (cf. below).[8,10,12] A behavior close to this limit is found, here, for *o*-terphenyl (cf. Fig. 6(c)). Contrarily, for hydrogen-bonded liquids like glycerol or PG (cf. Fig. 6(a)), the master curve bends upwards when linearity ceases to hold and accordingly one finds a large spectral separation $r \cong 40$ being much larger than the SED prediction.[10]

In Fig. 1 this situation is calculated for typical coupling constants but different spectral separation r. Here, applying Eq. (1), it is assumed that the rotational spectral density can be described by a Debye function (Eq. (6) with $\beta = 1$) and the translational spectral density by the FFHS model (Eq. (3)). Clearly, in the case of the hydrodynamic limit $r = 9$ (typical of *o*-terphenyl), the (blue) curve lies below the linear dotted line displaying the limiting low-frequency behavior while the (black) curve corresponding to $r = 50$ (close to the case of glycerol) lies well above. In the case of $r = 12$ (red curve), the linear behavior is apparently followed over a much larger frequency interval.

So far translational and rotational relaxation contributions have been specified by the spectral separation $r = \tau_{trans}/\tau_{rot}$. As mentioned, within the FFHS model $\tau_{trans} = d^2/2D$ and consequently $D\tau_{rot} = d^2/2r$ hold, i.e., the larger the $D\tau_{rot}$ the smaller is the spectral separation of translational and rotational contributions. Thus, instead of discussing the separation

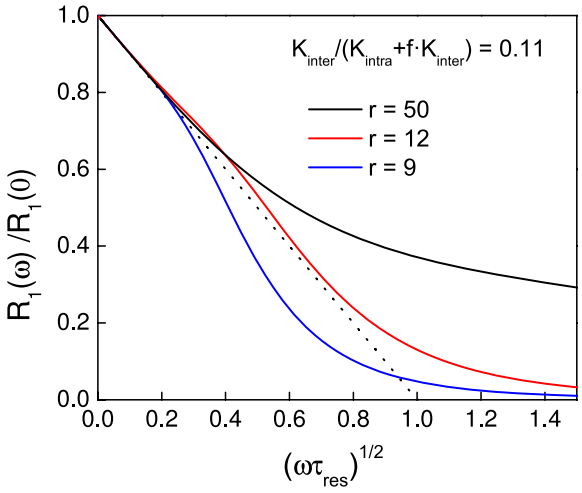

FIG. 1. Reduced relaxation rates, $R_1(\omega)/R_1(0)$ vs. $\sqrt{\omega\tau_{res}}$ calculated for different values $r = \tau_{trans}/\tau_{rot}$ characterizing the spectral separation of translational and rotational relaxation contributions. Dotted line: universal low-frequency dispersion law (cf. Eq. (10)).

parameter r, the quantity $D\tau_{rot}$ can be used to characterize the spectral separation of translational and rotational relaxation contributions.

Previously, as mentioned, covering a large temperature range, we extracted the rotational time constant $\tau_{rot}(T)$ by constructing master curves $\chi''(\omega\tau_{rot})$.[7,9,10,13] This approach assumes that independent of temperature the shape of the rotational correlation function as well as the spectral separation r do not change (usually a good approximation well above T_g).[25,26] In the present context, an alternative, more powerful approach (i.e., with less severe assumptions), can be pursued. As $R_1(0)$ is a linear combination of τ_{rot} and τ_{trans} (cf. Eq. (9)) while the coefficient in Eq. (7) $m = B/D^{3/2}$ only depends on D (cf. also Eq. (8)), one can gather information directly on the quantity $D\tau_{rot}$ when relating both parameters of the linear fit by Eq. (7), $R_1(0)$ and m, as follows:

$$\frac{R_1(0)}{m^{2/3}} = \frac{D\tau_{rot}(K_{intra} + f \cdot K_{inter}) + \frac{2}{9}K_{inter}d^2}{B^{2/3}}. \tag{12}$$

Assuming that spin density, N_H (cf. Eq. (4)), intramolecular coupling constant, K_{intra}, and the molecule's diameter, d (and therefore K_{inter}, cf. Eq. (4)) are constant in the considered temperature range, one can relate a temperature or concentration trend in $R_1(0)/m^{2/3}$ solely to a change in $D\tau_{rot}$. Absolute values on $D\tau_{rot}$ can be obtained when a low-temperature profile $R_1(\omega)$ (reflecting both rotational and translational relaxation contributions) is available, which allows to extract both τ_{rot} and D via fits employing Eqs. (1)–(6).[10] Besides τ_{rot} and D, the fit also yields K_{inter} (and therefore d) and the overall rotational coupling $K_{intra} + f \cdot K_{inter}$. With these parameters, Eq. (12) allows the calculation of $D\tau_{rot}$ (and τ_{rot}) for other datasets taken at higher temperatures where the relaxation dispersion due to rotation is not any more contained in the actual frequency window as one only needs the result of the linear fit of $R_1(\sqrt{\omega})$ at low frequencies, m and $R_1(0)$.

In conclusion, in a single experiment FC ^{1}H NMR relaxometry allows to provide the quantity $D\tau_{rot}$ which specifies the

extent of spectral separation of the translational and rotational relaxation contributions. Assuming SED to hold, $D\tau_{rot}$ may be taken as a measure of the hydrodynamic radius R_H. Explicitly, the combination of the Stokes-Einstein-relation[22]

$$D = (k_B T)/(6\pi\eta R_H), \tag{13}$$

the Stokes-Debye relation

$$D_{rot} = (k_B T)/\left(8\pi\eta R_H^3\right), \tag{14}$$

and the definition of the rotational time constant of rank, l,

$$\tau_{rot}^{(l)} = \frac{1}{l(l+1)D_{rot}} \tag{15}$$

gives for $l = 2$ (NMR case)

$$D\tau_{rot} = 2/9 \cdot R_H^2. \tag{16}$$

A spectral separation $r = 9$ follows from Eqs. (13)–(15), $\tau_{trans} = d^2/(2D)$ and setting $d = 2R_H$. Within the FFHS model, which does not imply the validity of SED relations, $D\tau_{rot} = d^2/2r$ holds, as said. Although the hydrodynamic limit represented by these equations may be challenged for the motion of molecules, it is interesting to discuss actual numbers obtained as was done before.[21,22]

EXPERIMENTAL

The ^{1}H NMR spin-lattice relaxation experiments were performed with a (fast) FC relaxometer (Stelar Spinmaster FFC 2000), where the external magnetic field is electronically switched. The relaxometer covers a ^{1}H frequency range from $\nu = \omega/2\pi = 10$ kHz to 20 MHz while the switching time from high polarization field to relaxation field was about 3 ms. The relaxation time T_1 was determined by an exponential fit of the magnetization decay curve. The temperature was controlled by heating flowing air or evaporating liquid nitrogen. Temperature stability was ±0.3 K. The protonated chemicals propylene glycol, glycerol, and *o*-terphenyl were purchased from Aldrich, Germany, the deuterated components from CDN Isotopes, Canada, and used without further treatment. The mole fractions $x = x_{PG}$ of PG in chloroform-d_1 varied from $x_{PG} = 1.0$ (pure PG) to $x_{PG} = 0.4$ (4 mol PG to 6 mol chloroform-d_1) with steps of 0.1. The accuracy hereby was better than ±0.02.

RESULTS

We pursue two approaches to extract $\tau_{rot}(x,T)$ (and thus $D\tau_{rot}$). First, $\tau_{rot}(x,T)$ is taken from constructing susceptibility master curves $\chi''(\omega\tau_{rot})$ while $D(x,T)$ is determined analyzing the low-frequency dispersion along Eq. (7). The second approach applies a quantitative description of the full low-temperature profiles (reflecting translational and rotational contributions) along the lines delineated in the section on Theoretical Background. Thereby, the coupling constants K_{intra}, K_{inter}, and f are obtained and $D\tau_{rot}(x,T)$ can be directly accessed for all temperatures (cf. Eq. (12)) provided that m can be still determined from the low-frequency dispersion. With D determined independently again $\tau_{rot}(x,T)$ is obtained and can be compared to the values from the first approach. This will confirm our approach extracting $D\tau_{rot}(x,T)$ by the full profile analysis in order to characterize the vanishing association of the PG molecules in solution with chloroform.

Figure 2(a) shows the results of PG in chloroform at $T = 233$ K in terms of the relaxation rate $R_1(\nu)$ (with $\nu = \omega/2\pi$) while in Fig. 2(b) the corresponding susceptibility representation $\nu R_1(\nu)$ of the data is displayed. The latter figure, in particular, shows directly the influence of adding chloroform to PG: Because of the lower viscosity of chloroform as compared to PG, the dynamics get faster with decreasing x_{PG} as becomes obvious by the relaxation peak shifting to higher frequencies. This effect, of course, is absent in the case of glycerol-h_5/glycerol-d_8 mixtures.[10]

Figure 3(a) shows the susceptibility master curve $\chi''(\omega\tau_{rot})$ for pure PG in comparison with that for pure glycerol-h_5

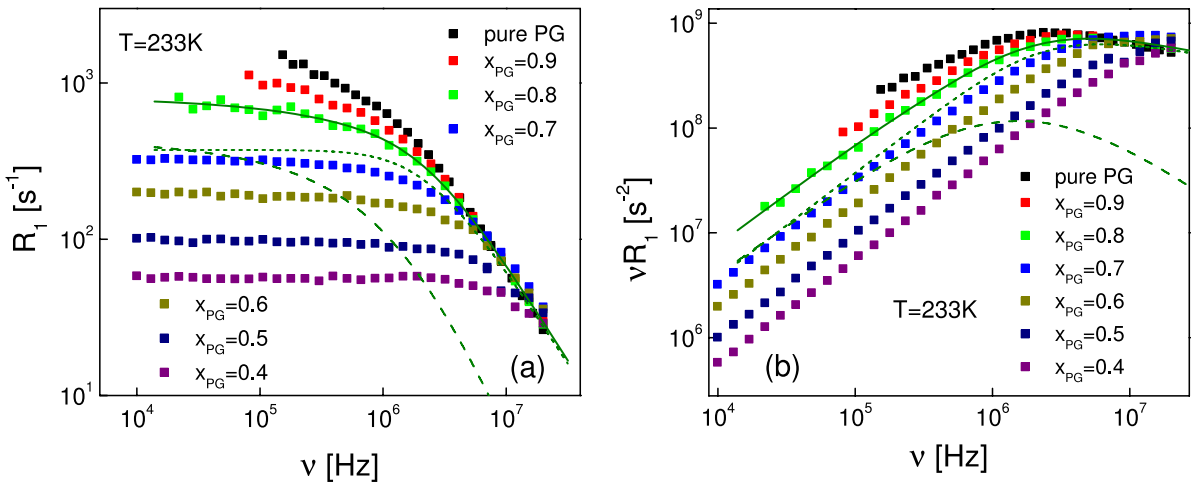

FIG. 2. (a) Relaxation rate dispersion, $R_1(\nu)$, as a function of frequency for different mole fraction x_{PG} of PG in chloroform-d_1 taken at $T = 233$ K; solid line: fit according to Eqs. (1)–(6), dotted line: rotational relaxation contribution (cf. Eq. (5)), dashed line: translational contribution (cf. Eq. (2)); fit parameters are listed in Table I. (b) Data of (a) in the susceptibility representation, $\nu R_1(\nu)$.

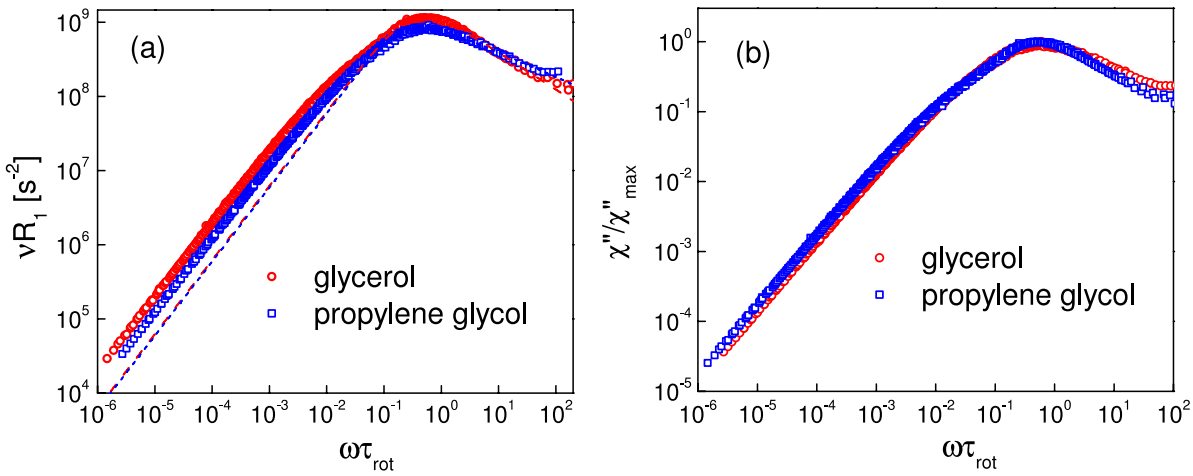

FIG. 3. (a) Susceptibility master curve, $\nu R_1(\omega\tau_{rot}) \propto \chi''(\omega\tau_{rot})$, for propylene glycol and glycerol-h_5, dashed lines: CD fits. (b) Data of (a) divided by the corresponding maximum value, χ''_{max}; low-frequency flanks virtually agree.

(from Ref. 10) as it is obtained by shifting the $R_1(T)$ data collected in a temperature range of 220K-330 K solely along the frequency axis and fixing one τ_{rot} at a temperature where a relaxation maximum allows an interpolation with a CD function. In addition to the main relaxation peak reflecting the reorientational dynamics in the liquid (α-process), in both liquids a pronounced but similar low-frequency shoulder is observed indicative of a strong translational relaxation contribution. On an absolute scale, the susceptibility data of PG and glycerol are somewhat different as expected due to different NMR coupling constants. In Fig. 3(b), the master curves are scaled to their maximum. Indeed, at $\omega\tau_{rot} < 1$ the shape of the master curves is very similar. At high frequencies ($\omega\tau_{rot} > 1$), the slope of the flank is somewhat different which is describable by a different stretching parameter when a CD function is applied to fit the peak region (dashed lines in Fig. 3(a)). The CD fits only account for the rotational contributions. As a consequence, they merely describe the maximum region and the high-frequency part of the master curves. Performing a quantitative analysis, we have shown that the r value is close to 40,[10] i.e., significantly larger than the hydrodynamic limit of $r = 9$.

In Fig. 4 the susceptibility master curves for the mixtures glycerol-h_5/glycerol-d_8 (a) and PG/chloroform-d_1 (b) for different concentrations are displayed. As the coupling constant decreases upon dilution, so does the relaxation peak. In addition, in the case of glycerol, one observes that the low-frequency shoulder continuously becomes smaller finally disappearing for the zero-concentration limit. As this limit reflects only intramolecular relaxation mediated by rotational dynamics, it can be interpolated by a CD function and the corresponding time constant well agree with those from dielectric spectroscopy.[3,10] In the case of PG/chloroform-d_1 mixtures, the shoulder observed for pure propylene glycol disappears already at intermediate concentrations (extrapolation to zero concentration is not possible). As discussed in the section on Theoretical Background, this is a fingerprint of a decreasing spectral separation of rotation and translational mediated relaxations. In other words, the translational relaxation contribution does not only decrease but also shifts towards the rotational peak at high frequency, i.e., translational-rotational coupling in terms of $r = \tau_{trans}/\tau_{rot}$ changes. Even another case is found for *o*-terphenyl in a mixture with its deuterated counterpart (Fig. 4(c)). Here, no low-frequency shoulder is recognized for all mole fractions as the spectral separation of translation and rotation is rather small; a value $r = 9$ has been found.[12] Thus, we conclude that in PG/chloroform-d_1, the r values changes from a value about 40 to about 9 at low PG concentration, and below we will discuss this trend as consequence of the dissolution of the hydrogen-bond network present in pure PG as well as in pure glycerol.

By constructing the master curves in Fig. 3, the corresponding rotational time constants $\tau_{rot}(x,T)$ are revealed and they are plotted in Fig. 5 (full circles). As expected, they do not change with dilution in the case of glycerol-h_5/glycerol-d_8 and *o*-terphenyl-h_{14}/*o*-terphenyl-d_{14}, while in the case of PG/chloroform-d_1 molecular rotation is accelerated by adding more and more chloroform. This is not surprising as the viscosity of chloroform is significantly lower than that of PG. In all the cases, non-Arrhenius temperature dependence is observed typical of dense liquids.[26]

The diffusion coefficient D is extracted from the low-frequency dispersion data by exploiting Eqs. (7) and (8), i.e., plotting the relaxation rate as a function of the square root frequency. As seen in Fig. 6(a), the low-frequency data of pure PG follow a linear relationship which extends to larger and larger frequencies the higher the temperature is. At high frequencies, the data lie above the linear low-frequency limit (dashed line). As demonstrated in Fig. 1, this is typical for a large separation of translational and rotational dynamics, i.e., a large r value. In contrast, in the case of PG with $x_{PG} = 0.4$ in chloroform-d_1, a quite different behavior is revealed (Fig. 6(b)). Now the data at high frequencies lie below the low-frequency limit. This is typical for small translational-rotational separation (cf. Fig. 1) close to $r = 9$. The behavior is similar to that of *o*-terphenyl (Fig. 6(c)). The linear low-frequency part provides $D(T,x)$ displayed in Fig. 7. In the case of glycerol and *o*-terphenyl for which FG NMR

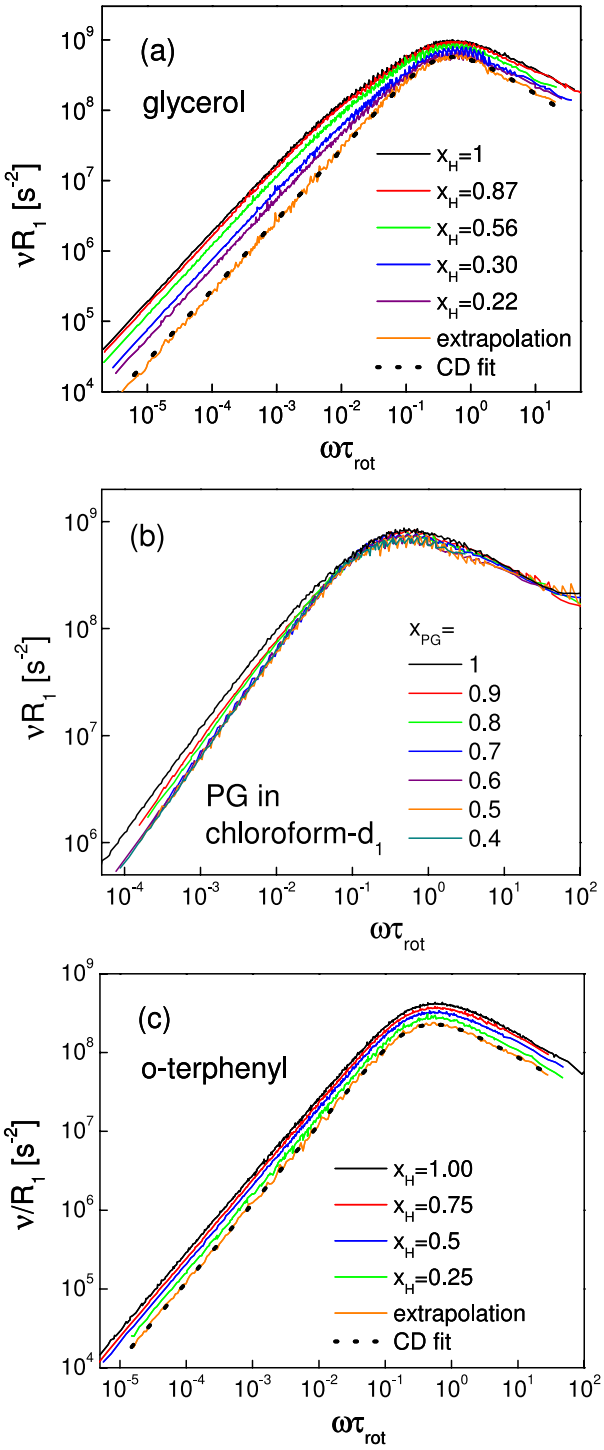

FIG. 4. (a) Susceptibility master curves, $\nu R_1(\omega\tau_{rot}) \propto \chi''(\omega\tau_{rot})$, for different mole fraction x_H of glycerol-h_5/glycerol-d_8 mixtures. (b) Analogous plot for different molar ratios x_{PG} of propylene glycol in chloroform-d_1. (c) Analogous figure for different ratios x_H of OTP-h_{14} in OTP-d_{14}. Solid orange line in (a) and (c): extrapolation $x \to 0$, dotted black line: fit by CD function.

diffusion data are available,[21,22] both data sets well agree and, as expected, no difference is found when diluted with their deuterated counterpart. For PG diluted with chloroform-d_1, the diffusion coefficient changes, specifically, at a given temperature D becomes higher with adding chloroform, again as expected.

The data in Fig. 6 can be rescaled to yield master curves for the relaxation rate, i.e., $R_1(\omega)/R_1(0)$ is plotted vs.

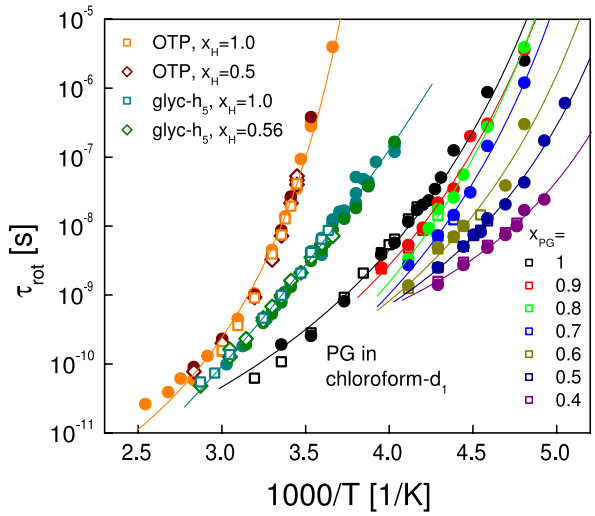

FIG. 5. Rotational time constants τ_{rot} versus reciprocal temperature obtained by construction of susceptibility master curves (solid circles) and via full analysis (Eq. (12); open symbols). Different systems are encoded by colors as indicated. In the case of *o*-terphenyl (OTP) and glycerol-h_5 mixtures no change with concentration is observed in contrast to propylene glycol (PG) in chloroform-d_1; solid lines: interpolations by Vogel-Fulcher-Tammann equation.

$\sqrt{\omega\tau_{res}}$ (cf. Theoretical Background). This is demonstrated in Fig. 8 where the master curves for glycerol-h_5/glycerol-d_8, *o*-terphenyl-h_{14}/*o*-terphenyl-d_{14}, and PG/chloroform-d_1 for different concentrations are shown. While for glycerol the disappearing low-frequency shoulder (reflecting translational relaxation contributions, cf. Fig. 3) is well recognized, in the case of *o*-terphenyl the shape of the master curve changes only weakly upon dilution. For the mixture PG/chloroform-d_1, qualitatively, the master curves change from a "glycerol case" (large r) at high PG concentration to a "*o*-terphenyl case" (small r) at high dilution. Thus, the change of the master curves $R_1(\omega)/R_1(0) = f(\sqrt{\omega\tau_{res}})$ in Fig. 7(c) reveals the change of translational-rotational coupling when the hydrogen-bond network liquid PG is diluted by chloroform which does not support hydrogen bonding.

In Fig. 9 the concentration dependence of $D(x)$ and $\tau_{rot}(x)$ are shown for PG/chloroform-d_1. As already noted, translational as well as rotational dynamics of PG accelerate upon dilution with chloroform. Yet, the effect appears to be stronger in D than in τ_{rot}. This is best recognized when the product $D\tau_{rot}(x,T)$ is plotted as a function of temperature as is done in Fig. 10 where a change of $D\tau_{rot}$ with x_{PG} is obvious. These results will be discussed below after having determined $D\tau_{rot}$ by the second approach covering a larger temperature range.

In order to obtain $\tau_{rot}(T)$, in a first approach, we took recourse to the construction of the master curves $\chi''(\omega\tau_{rot})$. Thereby, the product $D\tau_{rot}$ is accessible. As described in the section Theoretical Background, another approach is possible, i.e., one attempts to fully interpolate the relaxation profiles to get access to the coupling constants which then allow to directly calculate $D\tau_{rot}$ along Eq. (12). A low-temperature profile $R_1(\omega)$, containing dispersion due to both rotation as well as translation, can be fitted by applying Eqs. (1)–(6)—see full line in Fig. 2(a) for $x_{PG} = 0.8$ as an example. Explicitly, the spectral

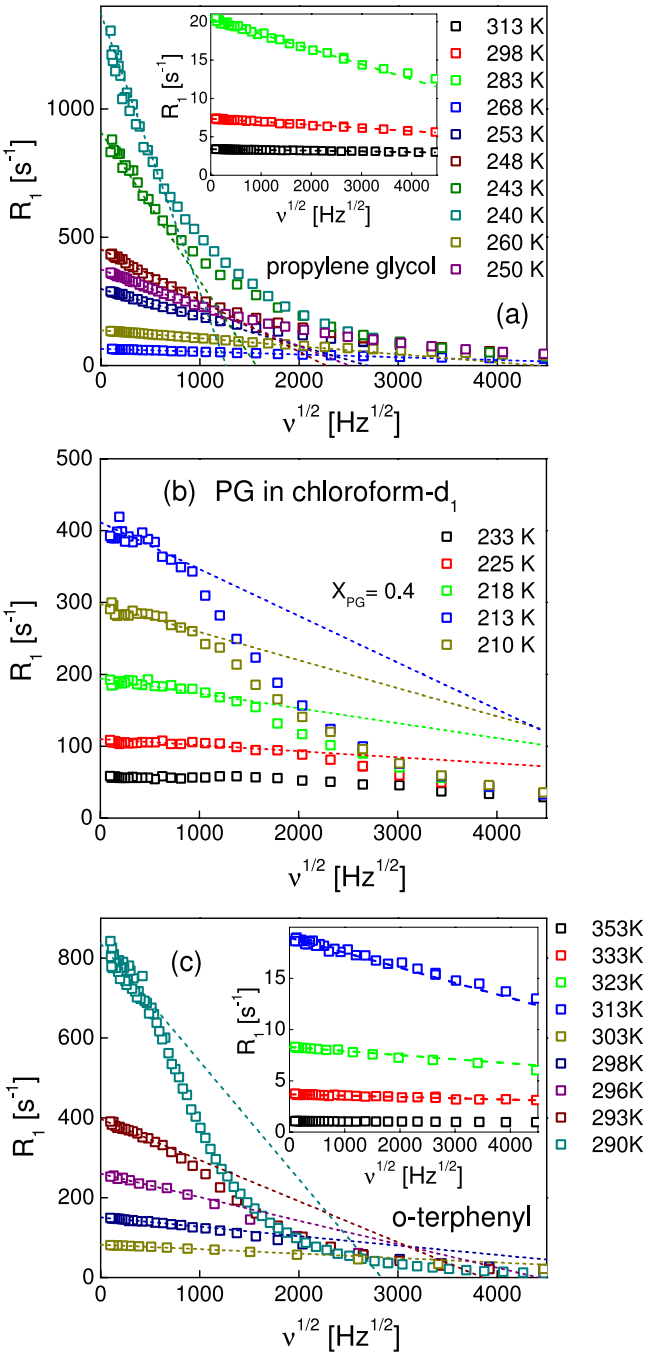

FIG. 6. (a) Relaxation rate versus square root of frequency of pure PG for different temperatures, inset: blowup for highest temperatures; dotted lines: linear low-frequency fits along Eq. (7). (b) Analogous data for PG in chloroform-d_1 with a mole fraction $x_{PG} = 0.4$. (c) Data for pure o-terphenyl.

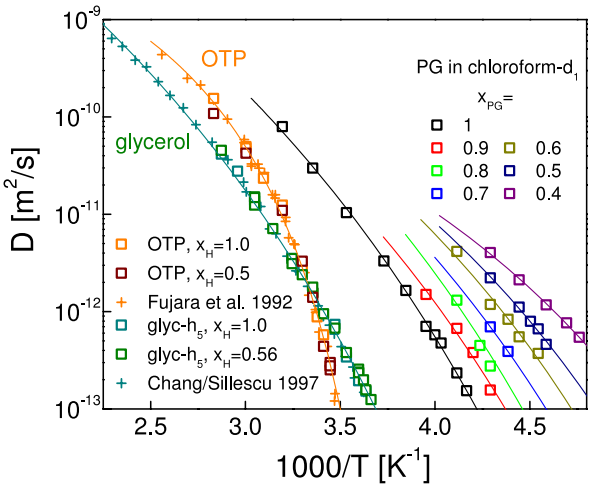

FIG. 7. Self-diffusion coefficient D for different mole fractions x_{PG} of PG/chloroform-d_1 mixtures, and for comparison, glycerol-h_5/glycerol-d_8[10] and o-terphenyl (OTP)/o-terphenyl-d_{14}[12] for different x_H versus inverse temperature as derived from the low-frequency behavior of $R_1(\sqrt{\nu})$ via Eq. (8). For comparison, D values from field gradient NMR data of pure OTP (Fujara *et al.*[21]) and of pure glycerol (Chang and Sillescu[22]) are included.

density provided by the FFHS model (translation) and by a CD function (rotation) are used, and the fit to $R_1(\omega)$ yields K_{inter} (and therefore d, cf. Eq. (4)) and the overall rotational coupling $K_{intra} + f \cdot K_{inter}$. In addition, we apply the constraint for K_{inter} $\propto \cdot x$ while K_{intra}, d, and f are assumed to be constant. Note, that the parameter B in Eq. (8) contains only physical constants. In Fig. 2(a), the decomposition in rotational and translational relaxation contributions is included. The dotted line reflects the rotational contribution (cf. Eqs. (5)–(6)) and the dashed line the translational contribution (cf. Eqs. (2)–(4)). The fit parameters are listed in Table I. With these parameters, one can derive $D\tau_{rot}$ for every profile taken at any other temperatures via Eq. (12), as long as the linear low-frequency behavior of $R_1(\sqrt{\omega})$ is still covered by the experimental data. The low-frequency limit provides the two parameters, $R_1(0)$ and m. Via $D\tau_{rot}$ the approach also gives access to τ_{rot}. The results of this analysis are shown in Fig. 5 as square symbols. In all cases, they agree well with the results obtained via the construction of master curves depicted as circle symbols. Thus, as D is extracted independently from the low-frequency dispersion, the quantity $D\tau_{rot}$ reflects only the differently determined τ_{rot} and, given their small difference revealed in Fig. 5, the corresponding $D\tau_{rot}$ values do not differ significantly among the two approaches and in what follows, we stick to the second approach providing $D\tau_{rot}$ via using the NMR coupling constants, i.e., via Eq. (12).

The results for $D\tau_{rot}(x,T)$ extracted by this method are included in Fig. 10. While in the case of glycerol, $D\tau_{rot}$ is virtually concentration independent yet with a weak trend to decrease at low temperature, a strong concentration dependence is seen for the mixtures PG/chloroform-d_1; the product $D\tau_{rot}$ increases by a factor 2 from $x_{PG} = 1$ to $x_{PG} = 0.4$. As already anticipated along with an increase of $D\tau_{rot}$(x), the spectral separation r becomes significantly smaller (cf. last column in Table II). Unlike the construction of the master curves, which relies on the applicability of FTS, i.e., on the invariability of the spectral separation of translational and rotational dynamics with temperature, the present analysis may even yield variation of $D\tau_{rot}$ as a function of temperature (cf. case of glycerol). The analysis only requires $K_{intra} + f \cdot K_{inter}$ and K_{inter} (and thus d) to be assumed constant with temperature. On the one hand, these parameters are based on molecular structure like the spin eccentricity, f, the distance of closest approach, d, and the intramolecular coupling K_{intra}, and on the other hand, on the density, ρ, of the liquid as $K_{inter} \propto N \propto \rho$. Both properties change if at all only weakly with temperature.

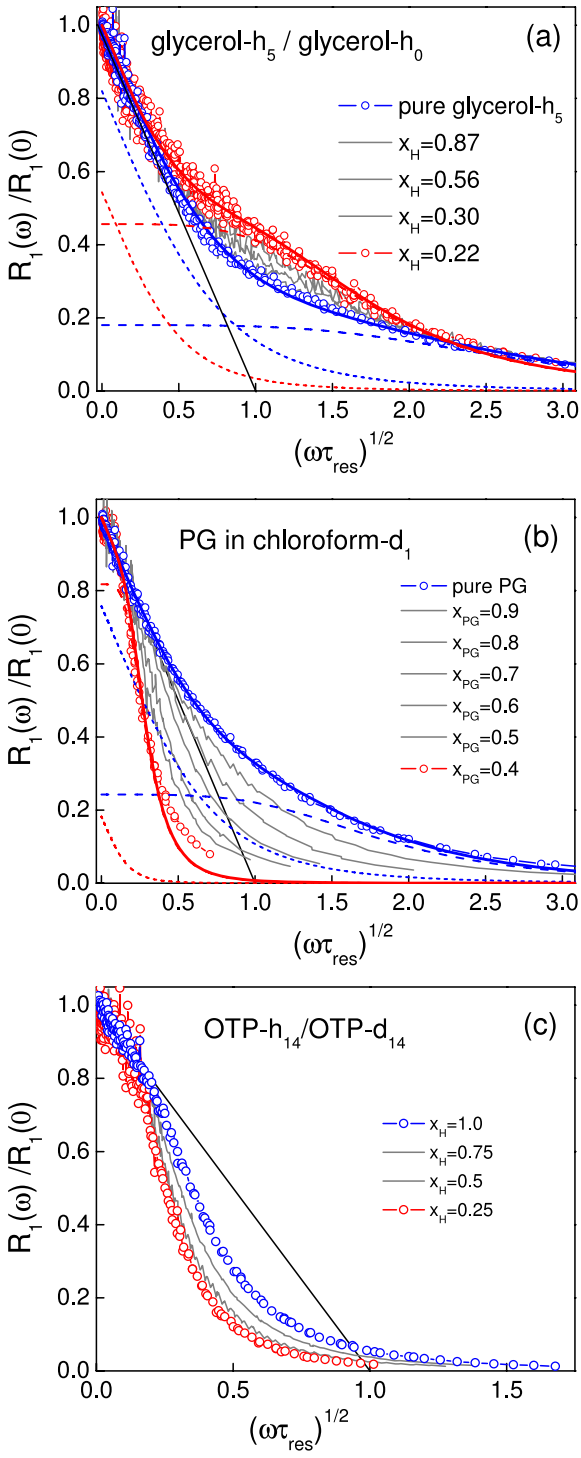

FIG. 8. (a) Master curves of the rescaled relaxation rate (collapsing dispersion data from different temperatures) as a function of square root of reduced frequency for glycerol-h_5/glycerol-d_8 mixtures with different mole fractions x_H; black solid line: low-frequency limit, blue (x_H = 1) and red solid lines (x_H = 0.22): fits employing a Debye function for the rotational part (dashed line) and the FFHS model for the translational part (dotted line); data taken from Ref. 10. (b) Analogous data for PG dissolved in chloroform-d_1, and (c) for *o*-terphenyl (OTP); data taken from Ref. 12.

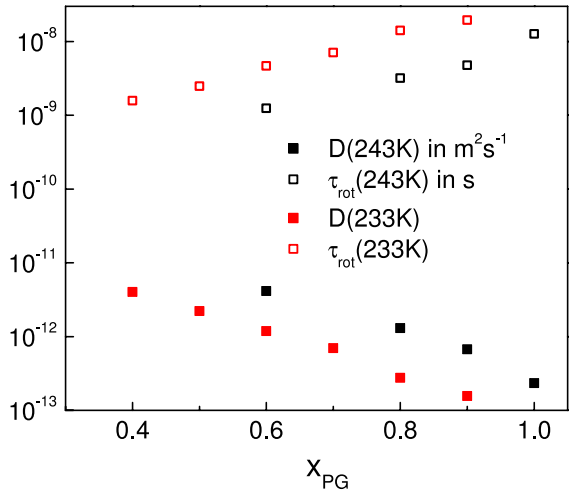

FIG. 9. Concentration dependence of rotational time constant τ_{rot} (open squares) and the self-diffusion coefficient D (solid squares) in the mixture propylene glycol/chloroform-d_1 at T = 243 K (black symbols) and T = 233 K (red symbols).

DISCUSSION

Two distinct approaches have been introduced which allow to extract consistently the product $D\tau_{rot}$ from the dispersion profiles measured by FC ^{1}H NMR relaxometry. Since ^{1}H relaxation reflects both translational and rotational dynamics via inter- and intramolecular relaxation pathways, no recourse to a second experimental method is needed. The quantity $D\tau_{rot}$ is a measure of the square of the hydrodynamic radius, or within the FFHS model, for which $D\tau_{rot} = d^2/2r$ holds, a measure of the spectral separation $r = \tau_{trans}/\tau_{rot}$. This can be exploited to monitor the changes of $D\tau_{rot}(x,T)$ in solution which reflect changes in molecular association while the separate quantities $D(x,T)$ and $\tau_{rot}(x,T)$ probe the change of the time scale of translational and rotational dynamics, respectively.

Specifically, the spectral separation of translational and rotational dynamics in terms of the product $D\tau_{rot}$ is unaffected in solution of glycerol-h_5 with its deuterated counterpart, as expected, since the solution structure does not change. The same holds for *o*-terphenyl-h_{14}/*o*-terphenyl-d_{14} mixtures. Still, in the case of glycerol, a slight rise of $D\tau_{rot}$ with temperature is observed, which is in agreement with literature data (cf. Fig. 10(a)).[21,29–34] However, at temperatures below $T \cong 1.2T_g$, not covered in this work, a distinctive rise is expected, which is commonly phrased as "breakdown of translational-rotational coupling due to enhanced translation."[21,22] The comparatively marginal variation of $D\tau_{rot}$ in the fluid and moderately viscous (super-cooled) regime basically confirms qualitatively the SED relation. In contrast, when PG is diluted with (deuterated) chloroform, a molecule not supporting hydrogen bonding, the value of $D\tau_{rot}$ significantly increases with concentration which indicates an increase of the (effective) hydrodynamic radius in the mixture or, equivalently, a decrease in the spectral separation r.

As shown in Table II, for pure PG, the mean value of $D\tau_{rot}$ yields $R_H = 0.12$ nm and $R_H = 0.17$ nm for PG/chloroform-d_1 at $x_{PG} = 0.6$-0.4. For the comparatively large molecule *o*-terphenyl a high value $R_H = 0.21$ nm and for glycerol a rather small value $R_H = 0.09$ nm is found. Table II also compares R_H with the molecule's diameter, d, obtained from the full fits of $R_1(\omega)$ with the FFHS model and the CD function. The relationship $R_H \cong d/2$ only holds for *o*-terphenyl and

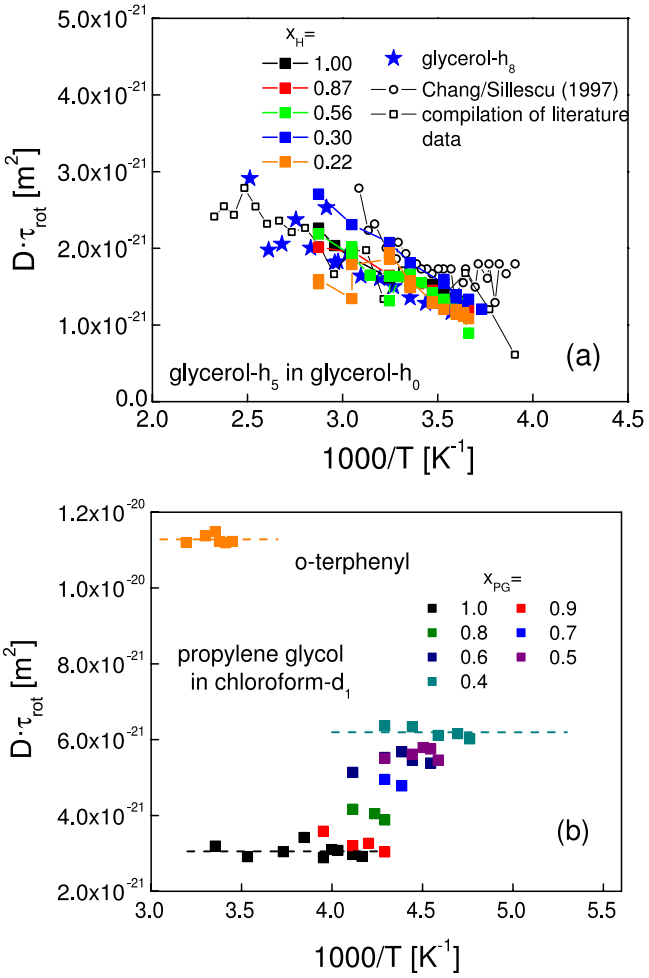

FIG. 10. (a) The product $D\tau_{rot}$ for glycerol-h$_5$ in glycerol-h$_0$ (solid squares) and for glycerol-h$_8$[12] (blue stars). For comparison, data from Ref. 22 included (open circles), further data extracted from the literature (Refs. 29–34). (b) Analogue data for the mixtures propylene glycol/chloroform-d$_1$ and for *o*-terphenyl.

PG in chloroform-d$_1$ with $x_{PG} = 0.6$, while for pure PG and glycerol R_H yields comparatively small values. In the case of *o*-terphenyl and PG in the mixture ($x_{PG} = 0.6$-0.4), this is consistent with $r \cong 9$, as this relationship is derived via identifying R_H with $d/2$ (cf. Eqs. (14) and (15)). In other words, the hydrodynamic model applies for non-associated molecules rather well. On the other hand, the strong deviation from $r \cong 9$ may be taken as an indication for associating molecules, as is the case of the hydrogen-bond network forming liquids

TABLE II. Van-der-Waals radius, R_{vdW},[35] apparent hydrodynamic radius, R_H, derived from $D\tau_{rot}$ and the "radius of closest approach," $d/2$, obtained by fits employing Eqs. (1)–(6), for comparison: results from Ref. 22.

Liquid	R_{vdW} (nm)	R_H (nm)	$d/2$ (nm)	R_H^{trans} (nm)[22]	R_H^{rot} (nm)[22]
Glycerol	0.27	0.09	0.21	0.16	0.096
o-terphenyl	0.37	0.21	0.20	0.23	0.23
Propylene glycol	0.26	0.12	0.19		
Propylene glycol/deuterated chloroform, $x_{PG} = 0.4$	0.26	0.17	0.19		

glycerol and propylene glycol. We conclude that in the mixture of PG with chloroform not only the dynamics is accelerated but also the hydrogen-bond network is essentially destroyed already at a concentration of $x_{PG} = 0.6$. Thus, the quantity $D\tau_{rot}$ (or r) allows to monitor the changes of the solution structure.

A discussion of the apparent hydrodynamic radius was also conducted by Chang and Sillescu.[22] Two separate values, R_H^{trans} and R_H^{rot}, with D from FG NMR experiments and τ_{rot} from ^{2}H NMR or dielectric measurements and viscosity data were given. For comparison, these values are included in Table II. The result of *o*-terphenyl, namely $R_H^{trans} \cong R_H^{rot} = 0.23$ nm is in good agreement with the value $R_H = 0.21$ nm extracted in this work. The identity of R_H^{trans} and R_H^{rot} means that the SED relations on translation and rotation simultaneously hold with the same apparent hydrodynamic radius, which goes along with $r \cong 9$ in our notation. As said, this situation is different for pure PG and glycerol. For glycerol, Chang and Sillescu reported $R_H^{trans} = 0.16$ nm and $R_H^{rot} = 0.096$ nm. The latter is again in good agreement with our result, $R_H = 0.09$ nm. The fact that in the case of glycerol $R_H^{trans} > R_H^{rot}$ (as well as in the case of pure PG) indicates that the SED relation does not apply in such associating liquids. The translational motion is comparatively slower than the rotational one, which is in the line that r exceeds the SED prediction of $r = 9$.

CONCLUSION

Exploiting the inter- and intramolecular relaxation contribution of ^{1}H spin-lattice relaxation rate $R_1(\omega)$, FC ^{1}H NMR yields rotational time constants $\tau_{rot}(T)$ and self-diffusion coefficients $D(T)$ (or corresponding time constants τ_{trans}) of liquids in a single experiment. The different evolutions of

TABLE I. Fit parameters for describing $R_1(\omega)$ of propylene glycol in chloroform-d$_1$ (Eqs. (1)–(6)) for different x_{PG} taken at appropriate (low) temperatures to cover both the translational and the rotational regimes (cf. Fig. 2).

x_{PG}	T (K)	$d/2$ (nm)	$K_{intra} + f \cdot K_{inter}$ (s^{-2})	τ_{rot} (s)	β	τ_{trans} (s)	r
1.0	243	0.19	$2.886 \cdot 10^{10}$	$1.00 \cdot 10^{-8}$	0.34	$3.56 \cdot 10^{-7}$	35
0.9	238	0.19	$2.876 \cdot 10^{10}$	$7.48 \cdot 10^{-9}$	0.32	$2.22 \cdot 10^{-7}$	30
0.8	233	0.19	$2.866 \cdot 10^{10}$	$1.30 \cdot 10^{-8}$	0.26	$2.98 \cdot 10^{-7}$	23
0.7	228	0.19	$2.856 \cdot 10^{10}$	$1.21 \cdot 10^{-8}$	0.27	$1.97 \cdot 10^{-7}$	16
0.6	220	0.19	$2.845 \cdot 10^{10}$	$1.46 \cdot 10^{-8}$	0.25	$1.98 \cdot 10^{-7}$	14
0.5	218	0.19	$2.834 \cdot 10^{10}$	$1.18 \cdot 10^{-8}$	0.25	$1.68 \cdot 10^{-7}$	14
0.4	210	0.19	$2.824 \cdot 10^{10}$	$1.07 \cdot 10^{-8}$	0.27	$1.49 \cdot 10^{-7}$	14

relaxation behavior between a liquid diluted with its deuterated counterpart, e.g., glycerol-h_5 in glycerol-d_8, and dilution with a chemically different deuterated substance, namely, PG in chloroform-d_1, has been examined. Upon adding chloroform-d_1, besides an acceleration of molecular dynamics of PG due to the lower viscosity of chloroform, a further significant difference is observed in terms of $D\tau_{rot}$ or $r = \tau_{trans}/\tau_{rot}$. The latter relations quantify the spectral separation of relaxation contributions from molecular translation and rotation in a liquid. While $D\tau_{rot}$ is independent of x_H in the case of glycerol-h_5/glycerol-d_8 or *o*-terphenyl/*o*-terphenyl-d_{14} adding chloroform-d_1 to PG increases $D\tau_{rot}$ which is equivalent with the reduction of the spectral separation of translational and rotational dynamics. Starting at $r \cong 40$, the spectral separation develops towards the behavior observed in *o*-terphenyl, namely $r \cong 9$. In contrast, in the case of glycerol and PG, there is a violation of the quantitative SED relation. For glycerol and PG, translational diffusion is significantly slower in relation to rotational motion than expected from the SED model, i.e., the SED relations for translation and rotation do not hold with a common hydrodynamic radius R_H. The phenomenon is attributed to the relevance of the hydrogen bond network in the solution structure for the case of glycerol and propylene glycol which in the latter case is steadily dissolved when chloroform is added. It appears that the hydrogen-bond network is already completely destroyed around a mole fraction of 60% PG. Generalizing these findings, via the quantity $D\tau_{rot}$, FC ^{1}H NMR allows to probe the network character of associating liquids.

ACKNOWLEDGMENTS

The authors appreciate financial support by the Deutsche Forschungsgemeinschaft (DFG) through the Grant No. RO 907/15.

[1]R. Kimmich and E. Anoardo, Prog. Nucl. Magn. Reson. Spectrosc. **44**, 257 (2004).
[2]D. Kruk, A. Herrmann, and E. A. Rössler, Prog. Nucl. Magn. Reson. Spectrosc. **63**, 33 (2012).
[3]R. Meier, D. Kruk, and E. A. Rössler, ChemPhysChem **14**, 3071 (2013).
[4]O. Lips, A. F. Privalov, S. V. Dvinskikh, and F. Fujara, J. Magn. Reson. **149**, 22 (2001).
[5]B. Kresse, A. F. Privalov, and F. Fujara, Solid State Nucl. Magn. Reson. **40**, 134 (2011).
[6]B. Kresse, M. Hofmann, A. Herrmann, E. R. Rössler, and F. Fujara, Solid State Nucl. Magn. Reson. **59-60**, 45 (2014).
[7]A. Herrmann, B. Kresse, J. Gmeiner, A. F. Privalov, D. Kruk, F. Fujara, and E. A. Rössler, Macromolecules **45**, 1408 (2012).
[8]A. Abragam, *The Principles of Nuclear Magnetism* (Clarendon Press, Oxford, 1961).
[9]D. Kruk, R. Meier, and E. A. Rössler, J. Phys. Chem. B **115**, 951 (2011).
[10]R. Meier, D. Kruk, J. Gmeiner, and E. A. Rössler, J. Chem. Phys. **136**, 034508 (2012).
[11]D. Kruk, R. Meier, and E. A. Rössler, Phys. Rev. E **85**, 020201 (2012).
[12]R. Meier, D. Kruk, A. Bourdick, E. Schneider, and E. A. Rössler, Appl. Magn. Reson. **44**, 153 (2012).
[13]R. Meier, A. Herrmann, M. Hofmann, B. Schmidtke, B. Kresse, A. F. Privalov, D. Kruk, F. Fujara, and E. A. Rössler, Macromolecules **46**, 5538 (2013).
[14]J. F. Harmon, Chem. Phys. Lett. **7**, 207 (1970).
[15]Y. Ayant, E. Belorizky, J. Alizon, and J. Gallice, J. Phys. (Paris) **36**, 991 (1975).
[16]L. P. Hwang and J. H. Freed, J. Chem. Phys. **63**, 4017 (1975).
[17]C. A. Sholl, J. Phys. C: Solid State Phys. **14**, 447 (1981).
[18]J. P. Kintzinger and M. D. Zeidler, Ber. Bunsen-Ges. Phys. Chem. **77**, 98 (1973).
[19]P. Lindner, E. Rössler, and H. Sillescu, Macromol. Chem. Phys. **182**, 3653 (1981).
[20]M. Kehr, N. Fatkullin, and R. Kimmich, J. Chem. Phys. **126**, 094903 (2007).
[21]F. Fujara, B. Geil, H. Sillescu, and G. Z. Fleischer, Z. Phys. B: Condens. Matter **88**, 195 (1992).
[22]I. Chang and H. Sillescu, J. Phys. Chem. B **101**, 8794 (1997).
[23]Y. Ayant, E. Belorizky, P. Fries, and J. Rosset, J. Phys. (Paris) **38**, 325 (1977).
[24]J. P. Albrand, M. C. Taieb, P. Fries, and E. Belorizky, J. Chem. Phys. **75**, 2141 (1981).
[25]P. Lunkenheimer, U. Schneider, R. Brand, and A. Loidl, Contemp. Phys. **41**, 15 (2000).
[26]N. Petzold, B. Schmidtke, R. Kahlau, D. Bock, B. Micko, R. Meier, D. Kruk, and E. A. Rössler, J. Chem. Phys. **138**, 154501 (2013).
[27]S. Kariyo, C. Gainaru, H. Schick, A. Brodin, V. N. Novikov, and E. A. Rössler, Phys. Rev. Lett. **97**, 207803 (2006); Erratum: S. Kariyo, A. Herrmann, C. Gainaru, H. Schick, A. Brodin, V. N. Novikov, and E. A. Rössler, Phys. Rev. Lett. **100**, 109901 (2008).
[28]S. Kariyo, A. Brodin, C. Gainaru, A. Herrmann, J. Hintermeyer, H. Schick, V. N. Novikov, and E. A. Rössler, Macromolecules **41**, 5322 (2008).
[29]C. Gainaru, O. Lips, A. Troshagina, R. Kahlau, A. Brodin, F. Fujara, and E. A. Rössler, J. Chem. Phys. **128**, 174505 (2008).
[30]T. Blochowicz, A. Kudlik, S. Benkhof, J. Senker, E. A. Rössler, and G. Hinze, J. Chem. Phys. **110**, 12011 (1999).
[31]A. Brodin and E. A. Rössler, Eur. Phys. J. B **44**, 3 (2005).
[32]H. A. Posch, H. D. Dardy, and T. A. Litovitz, Ber. Bunsenges. Phys. Chem. **81**, 744 (1977).
[33]H. Dux and T. Dorfmüller, Chem. Phys. **40**, 219 (1979).
[34]B. Chen, E. E. Sigmund, and W. P. Halperin, Phys. Rev. Lett. **96**, 145502 (2006).
[35]J. T. Edward, J. Chem. Educ. **47**, 261 (1970).